

Communication

# Controlled Surface Morphology and Electrical Properties of Sputtered Titanium Nitride Thin Film for Metal–Insulator–Metal Structures

Viet Dongquoc <sup>1,†</sup>, Dong-Bum Seo <sup>1,2,†</sup>, Cao Viet Anh <sup>3</sup>, Jae-Hyun Lee <sup>4,5</sup> , Jun-Hong Park <sup>6</sup>   
and Eui-Tae Kim <sup>1,\*</sup> <sup>1</sup> Department of Materials Science & Engineering, Chungnam National University, Daejeon 34134, Korea<sup>2</sup> Thin Film Materials Research Center, Korea Research Institute of Chemical Technology (KRICT), 141 Gajeong-ro, Yuseong-gu, Daejeon 34114, Korea<sup>3</sup> Department of Electrical Engineering, Chungnam National University, Daejeon 34134, Korea<sup>4</sup> Department of Energy Systems Research, Ajou University, Suwon 16499, Korea<sup>5</sup> Department of Materials Science and Engineering, Ajou University, Suwon 16499, Korea<sup>6</sup> Department of Materials Engineering and Convergence Technology, Gyeongsang National University, Jinju 52828, Korea

\* Correspondence: etkim@cnu.ac.kr

† These authors contributed equally to this work.



**Citation:** Dongquoc, V.; Seo, D.-B.; Anh, C.V.; Lee, J.-H.; Park, J.-H.; Kim, E.-T. Controlled Surface Morphology and Electrical Properties of Sputtered Titanium Nitride Thin Film for Metal–Insulator–Metal Structures. *Appl. Sci.* **2022**, *12*, 10415. <https://doi.org/10.3390/app122010415>

Academic Editor: Leonarda Francesca Liotta

Received: 8 September 2022

Accepted: 12 October 2022

Published: 15 October 2022

**Publisher's Note:** MDPI stays neutral with regard to jurisdictional claims in published maps and institutional affiliations.



**Copyright:** © 2022 by the authors. Licensee MDPI, Basel, Switzerland. This article is an open access article distributed under the terms and conditions of the Creative Commons Attribution (CC BY) license (<https://creativecommons.org/licenses/by/4.0/>).

**Abstract:** Titanium nitride (TiN) is a material of interest for electrodes owing to its high-temperature stability, robustness, low-cost, and suitable electrical properties. Herein, we studied the surface morphology and electrical properties of TiN thin film deposited onto an Si/SiO<sub>2</sub> <100> substrate through direct current (DC) sputtering with a high-purity TiN target in an argon-gas environment. The electrical properties and surface morphology of TiN thin film significantly improved with increased source power and decreased working pressure. The improved electrical properties could be attributed to the suppressed secondary phase (Ti<sub>2</sub>N) formation and the reduced electron scattering on smoother surface. Consequently, high-quality TiN thin film with the lowest resistivity ( $\rho = 0.1 \text{ m}\Omega\cdot\text{cm}$ ) and the smallest surface roughness (RMS roughness,  $R_q = 0.3 \text{ nm}$ ) was obtained under the optimized condition. The TiN film was further used as the bottom electrode for a metal–insulator–metal (MIM) capacitor. Results demonstrated that the electrical properties of TiN film were comparable to those of noble-metal thin films. Therefore, the TiN thin film fabricated by DC sputtering method had excellent electrical properties and good  $R_q$ , indicating its potential applications in MIM capacitors and Si technology.

**Keywords:** titanium nitride; thin film; surface roughness; electrical properties; magnetron sputtering

## 1. Introduction

Titanium nitride (TiN) is a metal nitride known for its high thermodynamic stability, high corrosion resistance, low friction constant, low electrical resistivity, and high mechanical hardness [1]. Based on these characteristics, TiN is extensively used in the microelectronics industry as a diffusion barrier [2], antireflective coating [3], gate material [4], Schottky barrier contact [5], and adhesion layer [6]. In particular, TiN thin film can be utilized as an electrode in dynamic random-access memory cells and in the back end of line metal–insulator–metal (MIM) capacitor electrode integrated circuits (ICs) [7]. The electrode used in MIM capacitors should have low electrical resistivity, and low surface roughness. Several methods can be used to prepare TiN thin films, such as chemical vapor deposition (CVD) [8], plasma-enhanced CVD (PE-CVD) [9], low-pressure CVD (LP-CVD) [10], and atomic-layer deposition (ALD) [11]. In CVD, high temperature is needed to degrade the strength of tool substrates, and the residual stress of the film is high. Pinholes and carbon contamination may occur in films deposited by organometallic PE-CVD [12]. ALD is a

chemical technique always accompanied by a risk of residues being retained from the precursors. The films' impurity content depends on reaction completeness [13]. In physical vapor deposition (PVD) methods, the environment is much cleaner owing to the high vacuum used and the lack of precursor compounds with unwanted elements. The direct current (DC) magnetron-sputtering method was selected for this study because of its many advantages, including low cost, high purity, uniformity, and good control over stoichiometry. Deposition conditions such as argon content in the chamber, power, pressure, residual oxygen in the chamber, substrate temperature, and substrate bias are important parameters for obtaining high-quality TiN thin film in reactive sputtering. Ponon et al. reported that as-deposited TiN<sub>x</sub> resistivity gradually decreases with increased nitrogen flow rate during deposition [14]. Jin et al. fabricated a TiN<sub>x</sub> thin film on different types of substrate and reported that the resistivity of TiN<sub>x</sub> film is strongly influenced by substrate temperature, deposition time, working pressure, bias power, and Ar and N<sub>2</sub> flow rate [15]. Jeyachandran et al. showed that thickness and N<sub>2</sub> concentration strongly affect the electrical, optical, compositional, structural, and morphology properties of TiN thin films [16]. However, further systematic information on the correlation between sputtering process parameters and properties of TiN is required to produce TiN thin films for a low resistivity and optimized MIM structures. Moreover, a comprehensive study on the effects of operating pressure and source power to improve the quality of TiN thin films that can be used as an electrode material in advanced MIM capacitors and IC technologies has not yet been fully resolved.

Herein, we prepared TiN thin films on an Si/SiO<sub>2</sub> <100> substrate through the DC magnetron-sputtering method. The effects of source power and working pressure on the roughness surface and resistivity of TiN thin film were studied in detail. Our results demonstrated that the surface roughness and resistivity of TiN thin film can be strongly improved by increasing the source power and decreasing the working pressure. We can obtain high-quality of TiN thin film with low resistivity (0.1 mΩ·cm) and small surface roughness (RMS roughness, R<sub>q</sub> = 0.3 nm) by using 150 W bias power and 0.5 × 10<sup>-3</sup> Torr as the optimum sputtering conditions.

## 2. Experimental Section

Si/SiO<sub>2</sub> <100> substrates (2 × 2 cm<sup>2</sup>) were degreased with ultrasonic acetone and propanol for 15 min sequentially, rinsed with deionized water for 10 min, and dried in N<sub>2</sub> atmosphere. The TiN thin films were prepared by DC magnetron sputtering system at a base pressure less than 6 × 10<sup>-6</sup> Torr using a high-purity (99.5%) 2" diameter TiN target. The target-to-substrate distance was 100 mm for all depositions, and the rotation speed was 5 rpm. The TiN thin films were grown on Si/SiO<sub>2</sub> <100> substrates for 10 min in Ar gas at a flow rate of 30 standard cubic centimeter per minute (SCCM). To investigate the effect of source power, the TiN thin film was deposited at various source power (25, 50, 75, 100, 150, and 175 W). Subsequently, the working pressure was changed to 0.5, 1, 2, 3, and 5 mTorr at a fixed source power of 150 W to further investigate the effect of working pressure.

The surface morphology and thickness of TiN thin films were determined by field-emission scanning electron microscopy (FE-SEM; S-4800, Hitachi, Ibaraki, Japan). Surface roughness was analyzed by atomic force microscopy (AFM; Asylum Research, Oxford, UK, MFP-3D). The crystal structure of films was characterized by the X-ray diffraction (XRD, λ = 1.548 Å, Empyrean, Panalytical, Malvern, UK). Intrinsic electrical characterization of TiN thin film was compared using resistivity, which was measured with the four-point probe method (CMT-SR1000N). The MIM devices were fabricated with circular Ti (5 nm)/Au (200 nm) as a top electrode 150 μm in diameter formed on Si/SiO<sub>2</sub> <100>/TiN/Al<sub>2</sub>O<sub>3</sub> thin films by using a shadow mask. The electric properties of MIM capacitors were studied with a Keithley 4200A-SCS parameter analyzer.

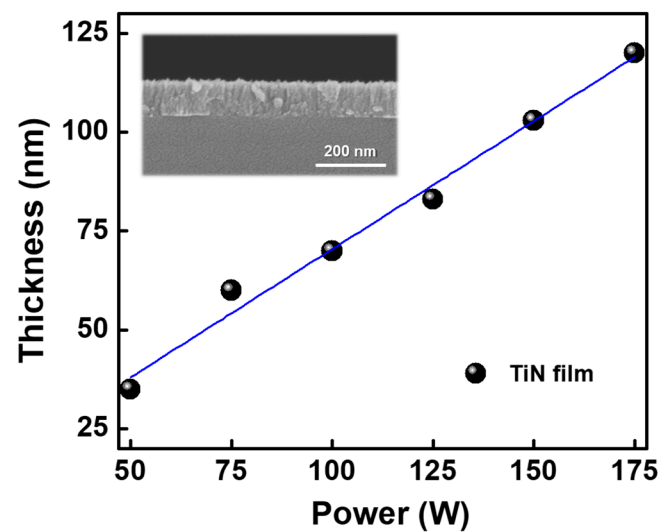
## 3. Results and Discussion

Figure 1 shows the thickness of the TiN thin film measured as a function of source power, which was adjusted from 50 W to 175 W. Thickness was found to increase linearly

with increased source power primarily because a greater sputtering power corresponded with stronger field strength among electrons. Consequently, the number of sputtered particles increased owing to the increased avalanche multiplication effect [17]. Accordingly, a faster sputtering rate corresponded with a greater thickness of TiN thin film that can be obtained with an increased source power under the same sputtering time. The thickness of TiN thin film measured as a function of source power was fitted by the function

$$Y = A_1 \times X + A_2 \quad (1)$$

where  $A_1$  is the deposition rate ( $A_1 = 0.548 \text{ nm/W}$ ),  $X$  is the source power, and  $A_2$  is a small offset ( $A_2 = 5.6 \text{ nm}$ ). The inset in Figure 1 shows the cross-sectional SEM image of TiN thin film on the Si/SiO<sub>2</sub> <100> substrate.



**Figure 1.** Variation in thickness of TiN thin film on the Si/SiO<sub>2</sub> <100> substrate with various source power.

Figure 2 shows the surface morphology of the as-deposited TiN thin films on the Si/SiO<sub>2</sub> <100> substrate as characterized by SEM. The TiN thin film deposited at a low source power of 50 W had relatively small dense particles with small void spacing and a smooth and uniform surface, as shown in Figure 2a. With increased source power, the grain size moderately expanded and the grain boundaries increased. This tendency became more obvious at higher source power (150 and 175 W), as displayed in Figure 2e,f. The inset images of Figure 2 show the cross-sectional morphology of TiN film at various source power and confirmed that the thickness of TiN film significantly increased with enhanced source power. The surface morphology of TiN thin film, in each case, was analyzed by SEM measurement for the corresponding sample. XRD study revealed the effect of source power on film crystallinity (Figure 3a). At a low source power of 50 W, only two peaks appeared at 43.6° and 51.2° of 2θ, corresponding to TiN and Ti<sub>2</sub>N, respectively. With increasing the source power, the peak intensity of Ti<sub>2</sub>N decreased while the TiN peaks became dominant. Above 100 W of source power, well-developed TiN peaks appeared at 36.8°, 42.7°, 62.1°, and 74.3°, corresponding to (111), (200), (220), and (311) orientation of TiN phase, respectively. A high source power formed a thick film with enhanced diffusion of nitrogen, resulting in predominant TiN phases [18]. However, the TiN peak position shift toward the lower diffraction angles at higher source power suggests the deficiency of the Ti component [19].

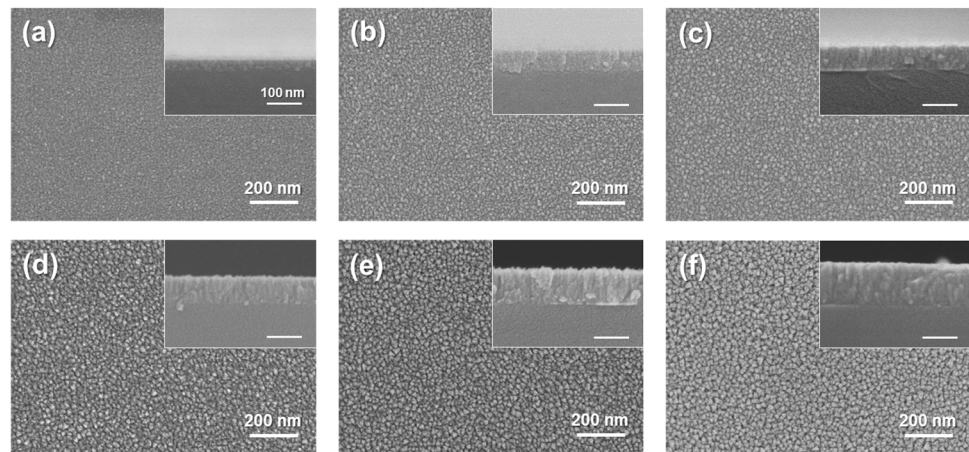


**Figure 2.** SEM surface morphology of TiN thin film deposited with various source power: (a) 50 W, (b) 75 W, (c) 100 W, (d) 125 W, (e) 150 W, and (f) 175 W, respectively. The inset presents a SEM image of TiN thickness.

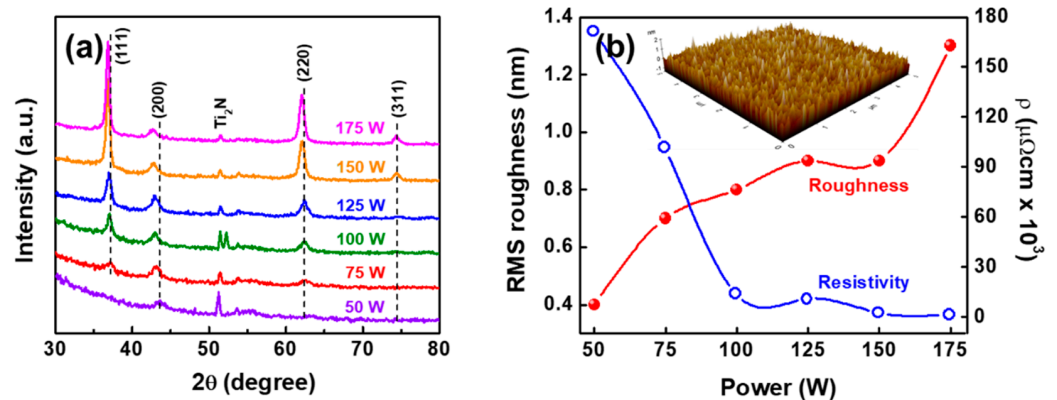


**Figure 3.** (a) XRD patterns, (b) RMS roughness ( $R_q$ ) and resistivity of TiN thin film on the Si/SiO<sub>2</sub> <100> substrate with various source power.

AFM analysis directly provided the surface roughness of TiN thin film from the three-dimensional AFM image, as shown in the inset of Figure 3b. The surface roughness (RMS roughness,  $R_q$ ) of TiN thin film strongly depended on the source power. At a lower source power (50 W), the film was very smooth and the  $R_q$  value was low (~0.4 nm).  $R_q$  continuously increased with enhanced source power, reaching 1.3 nm at 175 W of source power, as indicated in Figure 3b. A higher sputtering power and higher energy of incident ions or atoms caused clusters or grains to more easily aggregate and grow. Consequently, within a certain range of sputtering power, particle size was proportional to the sputtering power, which primarily explained the increase in  $R_q$  with increased the source power [17]. Moreover, the surface mounds gradually grew and the roughening phenomenon intensified with increased thickness of TiN thin film at a higher source power [20]. Figure 3b also shows the resistivity of TiN thin film as a function of source power. With enhanced source power from 50 W to 100 W, resistivity drastically decreased from 171 mΩ·cm to 14 mΩ·cm. Then, it gradually decreased with increased source power, reaching 1.47 mΩ·cm at 175 W. An abrupt decrease in resistivity was observed because the stoichiometric TiN deposited at the higher source power remained stable against oxidation [21], and the transformation from Ti<sub>2</sub>N phase to TiN phase. At high source power, the resistivity was low, but  $R_q$  was high. Accordingly, 150 W was selected for further studies to improve the surface roughness and electrical properties of TiN thin film. The surface morphology of TiN thin film on the Si/SiO<sub>2</sub> <100> substrate at various working pressure was investigated by SEM analysis (Figure 4).

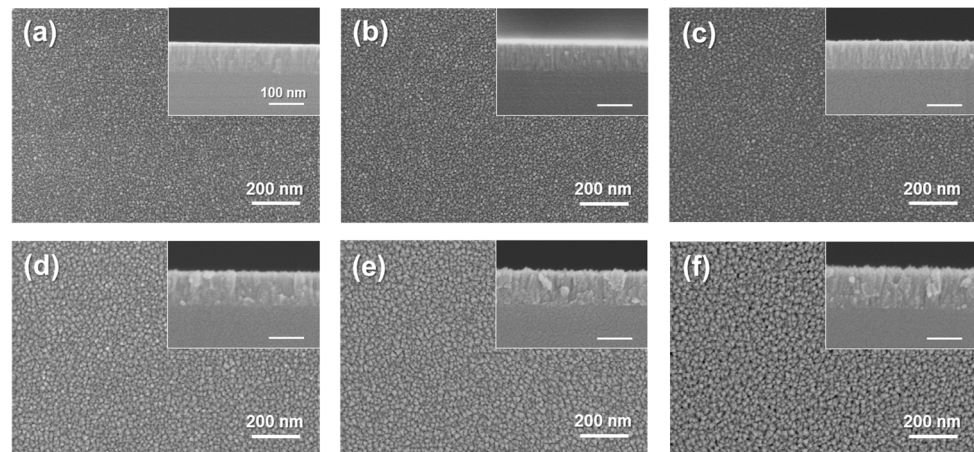


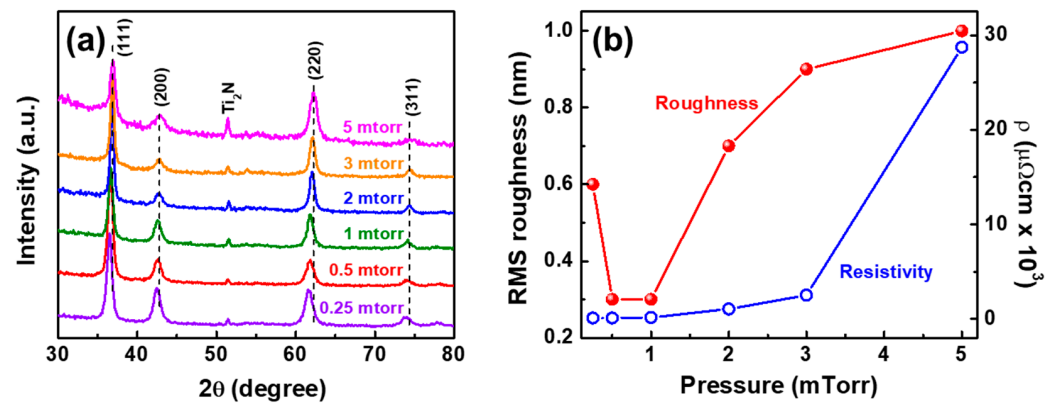
**Figure 4.** SEM surface morphology of TiN thin film deposited with various working pressure: (a) 0.25 mTorr, (b) 0.5 mTorr, (c) 1 mTorr, (d) 2 mTorr, (e) 3 mTorr, and (f) 5 mTorr. The inset presents a SEM image of TiN thickness.

At a higher working pressure ( $P_{\text{working}} = 5 \times 10^{-3}$  Torr) during films preparations, the evaporated TiN atoms presumably lost considerable energy through their numerous collisions with Ar atoms before they were deposited onto the Si/SiO<sub>2</sub> <100> substrate, resulting in insufficient growth of TiN film. With decreased working pressure, the surface morphology of TiN film drastically improved with small grain and narrow grain boundary. The insets of Figure 4 presented the cross-sectional microstructures of TiN film. As the working pressure was adjusted, film thickness slightly changed owing to the formation on the target surface a gas compound layer with a lower sputtering rate than metals [22]. Moreover, the cross-sectional images revealed growth morphology containing a columnar microstructure of TiN film at high working pressure, consistent with the characterization of the Zone T structure [23]. At lower working pressure ( $P_{\text{working}} \leq 1$  mTorr), columnar structures were not clearly observed, and TiN thin films grew well on the Si/SiO<sub>2</sub> <100> substrate.

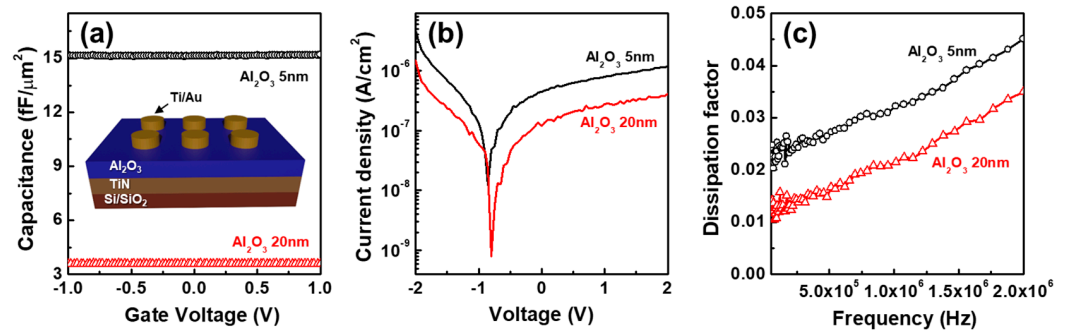
The XRD patterns of films deposited at various working pressures are shown in Figure 5a. With decreasing working pressure, the peak intensity of Ti<sub>2</sub>N decreased and the TiN peak position shifted toward the lower diffraction angles. A low working pressure seemed to enhanced diffusion of nitrogen, resulting in the transformation from Ti<sub>2</sub>N to TiN. Figure 5b shows that the  $R_q$  of TiN thin films continuously decreased from 1 nm to 0.3 nm at a working pressure of  $5 \times 10^{-3}$  and  $1 \times 10^{-3}$  Torr, respectively. However,  $R_q$  suddenly increased to 0.6 nm at a low working pressure of  $0.25 \times 10^{-3}$  Torr. A smoother surface helped reduce electron scattering and improve the conductivity of TiN film [14]. Consequently, the resistivity of TiN film abruptly decreased from 1.05 mΩ·cm to 0.14 mΩ·cm at a working pressure of  $2 \times 10^{-3}$  and  $1 \times 10^{-3}$  Torr, respectively, and then slowly decreased to 0.1 mΩ·cm at a  $P_{\text{working}}$  of about  $0.5 \times 10^{-3}$  Torr. The decreased resistivity can be attributed to the suppressed secondary phase (Ti<sub>2</sub>N) formation and the reduced electron scattering on smoother surface, which is also consistent with the results shown in Figure 3. The TiN thin films prepared under the optimum conditions at a source power of 150 W and working pressure of  $0.5 \times 10^{-3}$  Torr was utilized as a bottom electrode for MIM devices.

Figure 6a reveals the high-frequency (1 MHz) capacitance–voltage (C–V) characteristic of Al<sub>2</sub>O<sub>3</sub> MIM capacitors of various dielectric thickness, and the inset of Figure 6a shows the schematic of the MIM structure. The capacitance increased as the Al<sub>2</sub>O<sub>3</sub> became thinner, ranging within 3.5–15 fF/μm<sup>2</sup>. Among the various requirements for an analog MIM capacitor, leakage current density and dissipation factor are critical issues for MIM capacitor applications. Figure 6b shows that 5 nm and 20 nm Al<sub>2</sub>O<sub>3</sub> films exhibited excellent MIM leakage current density (approximately  $10^{-6}$  A/cm<sup>2</sup>) at 2 V. The dissipation factor at

1 MHz was also below 0.03 and 0.02 for the 5 nm and 20 nm  $\text{Al}_2\text{O}_3$  capacitors, respectively, as shown in Figure 6c.



**Figure 5.** (a) XRD pattern, (b) RMS roughness ( $R_q$ ) and resistivity of TiN thin film on the Si/SiO<sub>2</sub> <100> substrate with various working pressure.



**Figure 6.** (a) High-frequency (1 MHz) capacitance–voltage (C–V) curves, (b) leakage current density, and (c) dissipation factor as a function of frequency for MIM devices with various  $\text{Al}_2\text{O}_3$  thickness. The inset of (a) shows the schematic of MIM structure.

#### 4. Conclusions

The morphology and electrical properties of TiN thin films grown on Si/SiO<sub>2</sub> <100> substrates by using a DC sputtering system were investigated. The effects of source power and the working pressure on roughness and resistivity were systematically studied. The TiN thin films with suppressed secondary phase (Ti<sub>2</sub>N) formation remained stable against oxidation at a high source power, resulting in very low resistance. The smallest  $R_q$  value of 0.3 nm and the lowest resistivity of 0.10 m $\Omega$ -cm were obtained for the TiN thin film fabricated at a high source power (150 W) and low working pressure ( $0.5 \times 10^{-3}$  Torr). Moreover, we applied the MIM structure to the TiN thin film and confirmed that its electrical properties were comparable to those of noble-metal thin films. These results suggest that TiN films are potential application candidates in MIM capacitors and Si technology.

**Author Contributions:** Conceptualization, V.D. and E.-T.K.; Data curation, V.D., D.-B.S. and E.-T.K.; Formal analysis, V.D. and D.-B.S.; Funding acquisition, D.-B.S. and E.-T.K.; Investigation, V.D., D.-B.S. and C.V.A.; Methodology, V.D.; Supervision, E.-T.K.; Writing—original draft, V.D. and D.-B.S.; Writing—review and editing, J.-H.L., J.-H.P. and E.-T.K. All authors have read and agreed to the published version of the manuscript.

**Funding:** This work was supported by the National Research Foundation of Korea (NRF) grants funded by the Korea government (MSIT) (2020R1A4A4079397, 2021R1A2C1006241 and 2022R1C1C2005720). This work was also supported by “Regional Innovation Strategy (RIS)” through the National Research Foundation of Korea (NRF) funded by the Ministry of Education (MOE) (2021RIS-004, 2022H-01-02-08-005). This work was also supported by Samsung Electronics.

**Institutional Review Board Statement:** Not applicable.

**Informed Consent Statement:** Not applicable.

**Data Availability Statement:** Data are available in the main text.

**Conflicts of Interest:** The authors declare no conflict of interest.

## References

1. Groenland, A.W.; Wolters, R.A.M.; Kovalgin, A.Y.; Schmitz, J. On the leakage problem of MIM capacitor due to improper etching of titanium nitride. In Proceedings of the STW.ICT Conference 2010, Veldhoven, The Netherlands, 18 November 2010.
2. Yokoyama, N.; Hinode, K.; Homma, Y. LPCVD titanium nitride for ULSIs. *J. Electrochem. Soc.* **1991**, *138*, 190–195. [[CrossRef](#)]
3. Tompkins, H.G.; Sellers, J.A.; Tracy, C. An inorganic antireflective coating for use in photolithography. *J. Appl. Phys.* **1993**, *73*, 3932–3938. [[CrossRef](#)]
4. Lemme, M.C.; Efavi, J.K.; Mollenhauer, T.; Schmitdt, M.; Gottlob, H.D.B.; Wahlbrink, T.; Kurz, H. Nanoscale TiN metal gate technology for CMOS intergration. *Microelectron. Eng.* **2006**, *83*, 1551–1554. [[CrossRef](#)]
5. Dimitriadis, C.A.; Logothetidis, S.; Alexandrou, I. Schottky barrier contacts of titanium nitride on n-type silicon. *Appl. Phys. Lett.* **1995**, *66*, 502–504. [[CrossRef](#)]
6. Dauskardt, R.H.; Lane, M.; Ma, Q.; Krishna, N. Adhesion and debonding of multi-layer thin film structures. *Eng. Fract. Mech.* **1998**, *61*, 141–162. [[CrossRef](#)]
7. Lukosius, M.; Walczyk, C.; Fraschke, M.; Wolansky, D.; Richter, H.; Wenger, C. High performance metal–insulator–metal capacitors with atomic vapor deposited HfO<sub>2</sub> dielectric. *Thin Solid Films* **2010**, *518*, 4380–4384. [[CrossRef](#)]
8. Su, J.; Boichot, R.; Blanquet, E.; Mercier, F.; Pons, M. Chemical vapor deposition of titanium nitride thin films: Kinetics and experiments. *CrystEngComm* **2019**, *21*, 3974–3981. [[CrossRef](#)]
9. Charatan, R.M.; Gross, M.E.; Eaglesham, D.J. Plasma enhanced chemical vapor deposition of titanium nitride thin film using cyclopentadienyl cycloheptatrienyl titanium. *J. Appl. Phys.* **1994**, *76*, 4377–4382. [[CrossRef](#)]
10. Buiting, M.J.; Otterloo, A.F.; Montree, A.H. Kinetic aspects of the LPCVD of titanium nitride from titanium tetrachloride and ammonia. *J. Electrochem. Soc.* **1991**, *138*, 500–505. [[CrossRef](#)]
11. Heil, S.B.S.; Langereis, E.; Roozeboom, F.; van de Sande, M.C.M.; Kessels, W.M.M. Low-temperature deposition of TiN by plasma assisted atomic layer deposition. *J. Electrochem. Soc.* **2006**, *153*, 956–965. [[CrossRef](#)]
12. Lal, K.; Meikap, A.K.; Chattopadhyay, S.K.; Chatterjee, S.K.; Ghosh, M.; Baba, K.; Hatada, R. Electrical resistivity of titanium nitride thin films prepared by ion beam-assisted deposition. *Physica B* **2001**, *307*, 150–157. [[CrossRef](#)]
13. Leskelä, M.; Ritala, M. Atomic layer deposition chemistry: Recent developments and future challenges. *Angew. Chem. Int. Ed.* **2003**, *42*, 5548–5554. [[CrossRef](#)] [[PubMed](#)]
14. Ponon, N.K.; Appleby, D.J.R.; Arac, E.; King, P.J.; Ganti, S.; Kwa, K.S.K.; O’Neill, A. Effect of deposition conditions and post deposition anneal on reactively sputtered titanium nitride thin films. *Thin Solid Films* **2015**, *578*, 31–37. [[CrossRef](#)]
15. Jin, Y.; Kim, Y.G.; Kim, J.H.; Kim, D.K. Electrical properties of DC sputtered titanium nitride films with different processing conditions and substrates. *J. Korean Ceram. Soc.* **2005**, *7*, 455–460.
16. Jeyachandran, Y.L.; Narayandass, S.K.; Mangalaraj, D.; Areva, S.; Mielczarski, J.A. Properties of titanium nitride films prepared by direct current magnetron sputtering. *Mater. Sci. Eng. A* **2007**, *445–446*, 223–236. [[CrossRef](#)]
17. Zhou, C.; Li, T.; Wei, X.; Yan, B. Effect of the sputtering power on the structure, morphology and magnetic properties of Fe films. *Metals* **2020**, *10*, 896. [[CrossRef](#)]
18. Aghajani, H.; Motlagh, M.S. Effect of temperature on surface characteristics of nitrogen ion implanted biocompatible titanium. *J. Mater. Sci.-Mater. Med.* **2017**, *28*, 29. [[CrossRef](#)]
19. Chinsakolthanakorn, S.; Buranawong, A.; Chiyakun, S.; Limsuwan, P. Effects of titanium sputtering current on structure and morphology of TiZrN films prepared by reactive DC magnetron Co-sputtering. *Mater. Sci. Appl.* **2013**, *4*, 689–694. [[CrossRef](#)]
20. Hu, C.; Cai, J.; Li, Y.; Bi, C.; Gu, Z.; Zhu, J.; Zang, J.; Zheng, W. In situ growth of ultra-smooth or super-rough thin films by suppression of vertical or horizontal growth of surface mounds. *J. Mater. Chem. C* **2020**, *8*, 3248–3257. [[CrossRef](#)]
21. Logothetidis, S.; Meletis, E.I.; Stergioudis, G.; Adjaottor, A.A. Room temperature oxidation behavior of TiN thin film. *Thin Solid Films* **1999**, *338*, 304–313. [[CrossRef](#)]
22. Han, Z.; Tian, J.; Lai, Q.; Yu, X.; Li, G. Effect of N<sub>2</sub> partial pressure on the microstructure and mechanical properties of magnetron sputtered CrN<sub>x</sub> films. *Surf. Coat. Technol.* **2003**, *162*, 189–193. [[CrossRef](#)]
23. Wu, Z.T.; Qi, Z.B.; Zhang, D.F.; Wei, B.B.; Wang, Z.C. Evaluating the influence of adding Nb on microstructure, hardness and oxidation resistance of CrN coating. *Surf. Coat. Technol.* **2016**, *289*, 45–51. [[CrossRef](#)]